Journal of
Composites Science

MDPI

Article

Synthesis of Supported Metal Nanoparticles (Au/TiO_2) by the Suspension Impregnation Method

Carolina Rodríguez-Martínez [1], Ángel Emilio García-Domínguez [1], Fernando Guerrero-Robles [1], Rafael Omar Saavedra-Díaz [1], Gilberto Torres-Torres [1], Carlos Felipe [2], Reyna Ojeda-López [3], Adib Silahua-Pavón [1] and Adrián Cervantes-Uribe [1,*]

[1] Centro de Investigación de Ciencia y Tecnología Aplicada de Tabasco (CICTAT), Laboratorio de Nanomateriales Catalíticos Aplicados al Desarrollo de Fuentes de Energía, Universidad Juárez Autónoma de Tabasco, Tabasco 86690, Mexico; dicaro.roma@hotmail.com (C.R.-M.); angel.emilio.gardo@gmail.com (Á.E.G.-D.); fgro.96@gmail.com (F.G.-R.); rafael.saavedra@ujat.mx (R.O.S.-D.); gilberto.torres@ujat.mx (G.T.-T.); adib.silahua@ujat.mx (A.S.-P.)

[2] Centro Interdisciplinario de Investigaciones y Estudios sobre Medio Ambiente y Desarrollo (CIIEMAD), Instituto Politécnico Nacional, Ciudad de Mexico 07340, Mexico; cfelipe@ipn.mx

[3] Departamento de Engenharia Química, Universidade Federal do Ceará, Fortaleza 60455-760, Brazil; iqrol_87@hotmail.com

* Correspondence: adrian.cervantes@ujat.mx

Received: 9 June 2020; Accepted: 7 July 2020; Published: 9 July 2020

Abstract: This work reports a new technique called "Suspension Impregnation Method" (SiM) as an alternative to the "Incipient Impregnation Method" (IiM) for the synthesis of noble metal (Au) nanoparticles. The SiM was used to synthesize gold nanoparticles supported by titanium oxide and compared with those of IiM. The reactor for the SiM technique was based on the principles of mixing, heat, and mass transfer of the suspension reactors and the metal particle synthesis was processed in situ under the oxidation reduction potentials. Three different conditions were established to observe the effect of pH on the size of the metal particles: acid (HCl), neutral (water) and alkaline (urea). The samples were characterized by nitrogen adsorption, X-Ray Diffraction (XRD), Inductively Coupled Plasma Optical Emission Spectrometry (ICP-OES), Thermogravimetric Analysis (TGA)/Differential Thermal Analysis (DTA), Transmission Electron Microscopy (TEM) and CO_2 adsorption. The surface area was slightly modified, and the average pore diameter was reduced in all materials. The structure of the titanium oxide was not altered. A deposit of organic material was detected in samples synthesized in alkaline medium for both methods. The pH influenced the formation of conglomerates in IiM and resulted in large particle sizes (3–9 nm). In contrast, an in situ reduction in the species in SiM resulted in smaller particle sizes than IiM (2–3 nm).

Keywords: suspension impregnation method; Au; TiO_2; nanoparticles; CO_2

1. Introduction

Nanoparticles (NP) are solid particles at the atomic or molecular scale, synthesized to take advantage of the properties presented by materials at this level and are usually larger than bulk solids. The activity of the metallic nanoparticles has been attributed to quantum effects [1], load transfer to and from the metal to the support or induction of the support [2], spillover of oxygen to and from the support [3] and oxidation states, as well as the low coordination of atoms in the nanoparticles [4]. Several of the above effects are likely to occur simultaneously only if the size is nanometric. The research areas of nanoparticles are diversified: optical and electronic properties (Ag) [5], hydrotreatment to improve biodiesel fuel (Pd) [6], glucose biosensors (Pt) [7], N_2O decomposition (Rh) [8], and selective

solar absorption (Ni) [9]. The advantages of particles at the nanometric level are diverse and their synthesis is of high relevance. Gold is an example of the properties at the nanometer level. It was believed that this metal had no activity and, for a long time, its use was ruled out. It was not until 1980 that Harua showed an ideal technique for the synthesis of stable and active gold particles smaller than 3 nm [10]. Valden et al. [11] studied the activity of gold nanoparticles (AuNP), and they argue that AuNPs with a diameter of 3 nm have the highest activity for CO oxidation; this can be attributed to the effect of the quantum size of the nanosized particles and the effect of load transfer with the carrier. In case of the decomposition (oxidation) of formic acid, the thermally activated catalytic decomposition gradually increases when increasing the number density of deposited and saturated AuNPs; the decomposition occurs near the interface of TiO_2 and AuNPs [12]. For CO oxidation, active Au sites are essential and play an important role in carrying out the reaction at lower temperatures. The nanoparticles help to create new adsorption sites at the interface for the adsorption and activation of O_2 molecules [13]. AuNPs' CO_2 adsorption capacities considerably increased by 20% in mercapto-silica (MOS) [14]. For all of the above reasons, there are a variety of methods or techniques for synthesizing nanoparticles. The most popular are impregnation [15] coprecipitation [16], deposition precipitation (DP) [17], chemical vapor phase decomposition [18], functionalized surface [19], liquid-phase deposition (LPD) [20], photodeposition (PD) [21], sol-gel dip coating [22], among others. The methods mentioned above involve at least two to three stages, independent of each other, to produce nanoparticles. The first stage involves the impregnation or deposition of the particles. The second stage involves washing of the material by the excess precipitant. The third stage involves heat treatments. Each stage considers various parameters that, in turn, affect the size of the metal particles and the efficiency of the charge, such as: type of support [23], precursor [24], concentration of the precursor [25], deposition time [26,27], temperature [27] and pH [27,28]. Furthermore, the further treatment of the catalyst, such as washing [29], calcination [30], reduction method [31] and even the rate of the addition of reducing agents [32] have also an impact on the properties of the final metal particles. The deposition precipitation (DP) method involves the addition of a precipitating agent into the solution of a support and a metal precursor [26]. Typically, DP is performed at relatively high temperature in order to enhance the extent and rate of the hydrolysis of the precursor. At the same time, the metal particle size decreases due to rapid nucleation and attraction between the anion and the positively charged oxide surface [30]. In addition to pH and temperature, there are also other parameters which affect the metal particle size and metal loading efficiency, such as reaction time [26], support [26], precipitation agent, etc. A washing stage is necessary to remove the excess precipitant, as the waste solution contains metal when the metal adsorption is not optimal and represents an extra burden to the environment. The impregnation method, which can be carried out either in dry [33] or wet states [34], is considered to be the cheapest and the simplest preparation method [10]. Principally, impregnation occurs in the following way: liquid containing dissolved metal species enters the pores. Thereafter, it diffuses into the pores and adsorbs. In the final drying step, the liquid is evaporated from the pores. The effect of pH during preparation on the metal particle size has not been intensively studied for the impregnation method [34–36]. The size of the nanoparticles is homogeneous by the deposit precipitation method, unlike the incipient imprecation method. However, the impregnation method does not generate residual solutions. The liquid-phase deposition method (LPD) allows for the preparation of Au dispersed on TiO_2 thin films [20]. The TiO_2 thin film containing Au^{III} ions is formed by the LPD method from a mixed solution of $(NH_4)_2TiF_6$, H_3BO_3 and $HAuC1_4$ under an ambient temperature and atmosphere. The Au content in the film is controlled by controlling the concentration of $HAuCl_4$ in the treatment solution. The heat treatment of the deposited film above 200 °C produced Au metal particles that were ca. 15 nm in diameter. The size distribution of the dispersed Au particles became broad as the heat treatment temperature increased [20]. The photodeposition method (PD) also uses $HAuCl_4$ solution. $HAuCl_4$ containing 8.5×10^{-4} M of gold and TiO_2 are adjusted at different pH values (pH 6, 9, 10, 11) using 0.1 M NH_4OH before illumination. The light source used is a 16-W UV lamp (wavelength = 254 nm) with

an irradiation time ranging from 10 min to 60 min with a stirring speed of 770 rpm. The nominal Au loading is 1 wt.%. During irradiation, the pH is controlled carefully at different pH values and the temperature of the solution is maintained. After irradiation, the solution is filtered and washed with deionized water until no Cl^- is detected within the $AgNO_3$ solution. The Au/TiO_2 catalyst has narrow Au particle size distribution and the particle size of Au was around 1.5 nm [21]. In the sol–gel method, the films are modified by addition colloidal Au solution in titanium peroxide sol to increase the photoresponse of TiO_2 in visible light. With the addition of 1–2% Au, the absorption wavelength of TiO_2 is shifted from 340 nm in UV to 450 nm in the visible region. This improved the photocatalytic activity. The average particle size of Au particles in these films is within the 15–20 nm range [22].

Based on the advantages of these methods, a method design was chosen that avoids the agglomeration of particles in solution, a heterogeneous size and residual solutions. This study proposes an alternative and efficient technique to synthesize nanoparticles, which was called the Suspension Impregnation Method (SiM). To support the scope of the technique, the results were contrasted by a conventional technique (incipient impregnation). Finally, the activity of the nanoparticles was tested in the CO_2 adsorption. Although it is true that the amounts adsorbed cannot be compared with mesoporous solids specially synthesized for CO_2 capture [37–41], the technique allows for the elucidation of the chemical activity of the materials synthesized in this work and proves that the proposed method (SiM) is a better alternative for TiO_2 impregnation with Au.

2. Materials and Methods

2.1. Description of the Equipment

The suspension impregnation method (SiM) is based on the principles of fluidized bed reactors. The operation of this type of reactor is based on the suspension of solid particles within the liquid, where they acquire a behavior like that of a fluid, while the gas acts as a diffuser. Bubbling fluidized bed reactors have several advantages, among which the following stand out: the speed of particle mixing confers simplicity and safety, the heat and mass transfer speeds between the gas and the particles are greater than other mixing systems, and a higher heat transfer capacity between a fluidized bed and an object. When considering the basic principles of operation, the slurry reactor was designed; see Figure 1. The reactor has gas (gas input) and liquid (solution input) inputs and an outlet for the solvent in the vapor phase (gas outlet). The pore bed has a diameter of 10 cm (pores of 0.05 mm diameter) at 12 cm from the "Solution Input". The input (solution input) has the function of giving access to the solution (dissolved precursor salt) and is at 4 cm from the "gas input". The reactor is made of glass with a thickness of 0.2 cm. It has a heating jacket and a thermocouple near the porous bed. The theoretical minimum fluidization flow (Q_{mf}) was calculated from Equations (1) and (2).

$$Q_{mf} = 60\pi\left(\frac{d}{2}\right)^2 V_{mf} \tag{1}$$

$$V_{mf} = \frac{d_p^2(\rho_s - \rho_l)g}{1650\mu} \tag{2}$$

Equation (1)—where d is the reactor diameter and V_{mf} is the minimum fluidization velocity obtained in Equation (2), where d_p is the particle diameter, ρ_s and ρ_l are the liquid and gas densities, respectively, g is the acceleration of gravity, and μ is the viscosity of gas [42].

All chemical reagents and solvents were analytical reagent grade and were used as received. All solutions were prepared with ultrapure water (18 M·Ω) from a Millipore Milli-Q system.

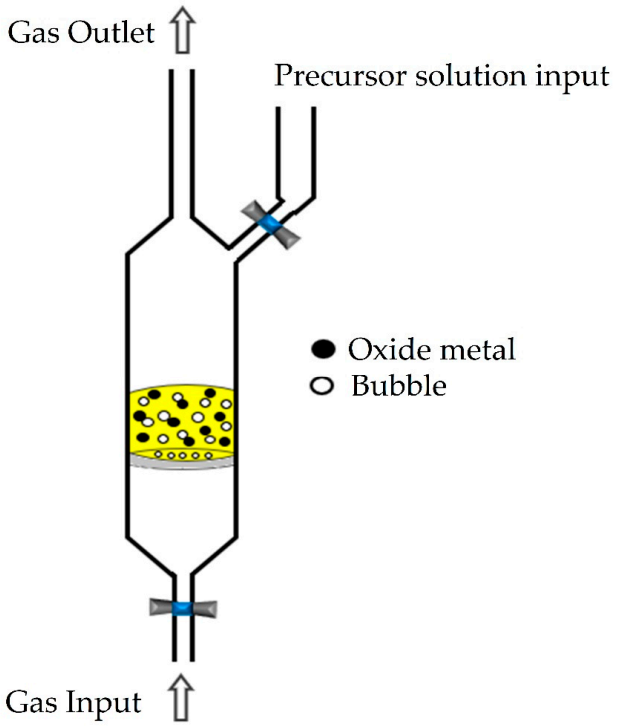

Figure 1. Diagram of the suspension reactor.

2.2. Synthesis of TiO_2

TiO_2 catalyst was obtained by the sol–gel method under acidic conditions and the synthesis was achieved as follows: a mixture of titanium isopropoxide (Aldrich, St. Louis, MI, USA, 97% by weight) and isopropanol (99.5%, Aldrich) was kept under constant stirring for 30 min; then, the pH of the mixture was adjusted to 3 with nitric acid (Aldrich, 70% by weight). Afterward, water was added dropwise to the mixture. The amount of water added was calculated at a molar ratio of 1:6 with respect to the alkoxide. The resulting sol was aged for 48 h, followed by the removal of the solvent by evaporation in a vacuum and then drying at 120 °C for 12 h. The xerogel was calcined at 500 °C for 2 h under an air atmosphere with a heating rate of 2 $°C^{-1}$.

2.3. Au/TiO_2 Synthesis by Impregnation

The conventional method known as insipient impregnation (IiM) was used to compare the results with the SiM method. In total, 2 g of sieved (0.7 mm) and degassed (nitrogen/300 °C, 30 min) TiO_2 was deposited in a round flask and brought into contact with a solution of dissolved $HAuCl_4$ (99.99%, Aldrich) (amount necessary to obtain 1% by weight of metallic gold). It was kept in vigorous agitation for 30 min; the solvent being stirred in a rotary evaporator. The dry sample was placed in a 120 °C oven for 12 h. It was then subjected to a reduction heat treatment in a hydrogen atmosphere with a heating ramp of 2 °C min^{-1} until it reached 350 °C. It remained in these conditions for 30 min. For this work, the pH of the solution was the only parameter that was changed. Three variations in the pH were determined: alkaline (urea), neutral (deionized water) and acid (HCl). The amounts of urea (Aldrich, 99%) and HCl (37% Aldrich) were 1:1 molar with respect to gold. The symbolism used for this investigation is: IAuTiB for the sample in alkaline pH, IAuTiA for the sample in acid medium and IAuTi for the sample without change.

2.4. Au/TiO_2 Synthesis by Suspension

In total, 2 g of the support (titanium oxide) was deposited in a porous bed screened with an average particle diameter of 0.7 mm. Subsequently, nitrogen was introduced through the “gas input”

section. The temperature was increased by 2 °C min^{-1} to 300 °C for 30 min to degas. The system was then allowed to cool to room temperature (35 °C) in nitrogen flow. The necessary amount of $HAuCl_4$ (99%, Aldrich) was dissolved to obtain 1% by weight of metallic gold. A volume of 5 mL of solution met the support and against gas (nitrogen) flow to promote agitation. After 30 min in agitation, the nitrogen was exchanged for hydrogen in a flow of 3.66 L h^{-1}. The temperature was increased at a rate of 2 °C min^{-1} to 350 °C. It remained at those conditions for 30 min. The same modification was established in the pH of the solution used in MiI. In the symbolism, only the "I" was exchanged for the "S", referring to MiS: SAuTiB, SAuTiA and SAuTi.

2.5. N_2 Adsorption (Specific Surface Area, Pore Diameter and Total Pore Volume)

Textural properties were determinate by N_2 adsorption-desorption. Total specific surface area, pore diameter and total pore volume of the AuTi materials was performed using the BET (Brunner–Emmet–Teller) equation (0.05–0.30 in relative pressure), NLDFT (Non-local Density Functional Theory) model and 0.95 in relative pressure, respectively. The results were obtained directly from the Autosorb Software. The analysis was performed in an ASAP 2020 instrument (Micromeritics) at 77 K (−196 °C). The samples were previously outgassed at 300 °C for 2 h to remove impurities.

2.6. X-Ray Diffraction (XDR)

Crystal phase identification for materials synthesized in different media was performed by X-ray diffraction in Bruker D8 Advance. The radiation used was CuKa with λ = 0.15406 nm. The analysis was carried out in a range of 2θ 20–70° with a step of 0.05° and a measurement time of 0.5 s per point.

2.7. Gold Concentration (ICP-OES)

Au concentration was obtained by optical emission spectroscopy with inductive coupling plasma using a 4200 DV equipment (PerkinElmer company, Waltham, MA, USA). For the preparation of the sample, 50 mg of catalyst was weighted and placed in a Teflon beaker, 3 mL of HF (48%, Aldrich) and 6 mL of a mixture of acid solution (4 mL of HNO_3 (70%, Aldrich) and 2 mL of HCl (37%, Aldrich)) were added. The mixtures were placed in an ultrasound bath at 75 °C for 1 h. After digestion, the solutions were filtered and calibrated in flasks of 50 mL with double distilled water.

2.8. Thermogravimetric Analysis (TGA) and Differential Thermal Analysis (DTA)

The experimental technique to determine the crystalline phase change temperatures of titanium oxide was thermogravimetric analysis (TGA)/differential thermal analysis (DTA). The thermal curves of TGA and DTA were obtained using a Diamond TG/DTA Thermogravimetric Differential Thermal Analyzer, PerkinElmer. The analysis of the samples was realized under a static air atmosphere and a heating ramp of 10 °C min^{-1} (UAM-I).

2.9. Transmission Electron Microscopy (TEM)

TEM was used to determine the size of the deposited metal particles, using dark field contrast. The analysis was performed using JEOL JEM-ARM200CF equipment, with acceleration voltages of 80–200 kV, using a Cold Field Emission Gun (CFEG) and an energy dispersive X-ray analyzer (EDX). For sample preparation, 1 μg sample was dissolved in 1 mL 2-propanol and immersed in an ultrasonic bath (Branson 2800 sonicator) for 15 min to achieve a better dispersion of the material. Finally, a drop of this dispersion was placed on a carbon film grid and allowed to dry for 24 h for further analysis.

2.10. HAADF-STEM

High-angle annular dark field (HAADF) and scanning transmission electron microscopy (STEM) analysis of the samples was performed in a JEE-2200FS transmission electron microscope with an

accelerating voltage of 200 kV. The microscope is equipped with a Schottky-type field emission gun and an ultra-high resolution (UHR). Configuration (Cs = 0.5 mm; Cc = 1.1 mm; point to point resolution = 0.19 nm); and an in-column omega-type energy filter. The samples were pulverized, suspended in isopropanol at room temperature and dispersed with ultrasonic agitation; then, an aliquot of the solution was dropped on a 3-mm diameter holey copper grid.

2.11. CO_2 Adsorption

CO_2 adsorption isotherms were measured on Autosorb 1 instrument (Quantachrome) until atmospheric pressure at 25 °C. The samples were previously outgassed at 300 °C for 2 h.

3. Results and Discussion

3.1. Sample Characterization

The isotherms shown in Figure 2A corresponds to type IV (A) according to International Union of Pure and Applied Chemistry (IUPAC) [43], typical of mesoporous solids, where the adsorption behavior in mesopores is determined by the adsorbent–adsorptive interactions. All samples showed hysteresis H1, characteristic of materials which exhibit a narrow range of uniform mesopores with open cylindrical pores and agglomerates of spherical particles of uniform distribution. When the TiO_2 is impregnated with Au, using the impregnation or suspension method, the isotherms show a displacement to the left, meaning a decrease in pore diameter. This behavior is appreciated in Figure 2B, where all modified materials decrease the average pore diameter. IAuTiA and SAuTiB present a more uniform pore size; however, SAuTiB moves into smaller pores, which means that the suspension method has been more efficient, and therefore that a greater amount of Au was impregnated. The pH in the impregnation synthesis slightly modified the textural properties (Table 1). In general, the BET area increases when the TiO_2 is modified, as the impregnation method in an acid medium presents a better surface area with respect to a basic medium. However, in the suspension method, as the pH has no significant effect, the value of the areas is practically the same. The total value increases, favoring a neutral pH. Considering the average pore diameter, the impregnated materials decrease the diameter; this means that a portion of the pores have been successfully modified.

Table 1. Textural properties and concentration, particle size and metal dispersion.

Sample	S_{BET} (m^2/g)	V_T (cm^3/g)	D_{NLDFT} (nm)	Au (wt%) [a]	Au Diameter (nm) [b]	D (%) [c]
TiO_2	47	0.169	13.9	-	-	-
IAuTi	58	0.185	11.3	0.98	3.96	30
IAuTiA	56	0.178	12.1	0.97	4.34	28
IAuTiB	52	0.175	12.1	0.98	9.35	13
SAuTi	54	0.191	14	0.91	3.07	42
SAuTiA	53	0.181	12.1	0.92	2.69	47
SAuTiB	53	0.154	11.3	0.91	3.67	35

[a] Percentage measured by ICP-OES. [b] Obtained by TEM images. [c] Metallic dispersion.

The results obtained by X-ray diffraction analysis of the synthesized samples are shown in Figure 3. The characteristic patterns of the anatase phase were identified 2θ 25.3, 37.8, 38.5, 48.1 and 53.8. The diffraction pattern corresponding to the crystalline phase brookite at 30.8° and rutile at the angle 27.4° of 2θ was also identified [44]. This mixture of phases is characteristic of catalysts synthesized from titanium isopropoxide [45]. Diffractions at 2θ 38.2, 44.4 and 64.58° are associated with the planes (111), (200) and (220) correspond to the cubic structure of metallic gold [46]. According to the results, the gold deposition by the impregnation and suspension methods did not affect the coexistence of the three crystalline phases of the titanium oxide. Furthermore, different intensity of gold peaks was observed in all samples. The samples with the highest diffraction intensity were those synthesized by IiM in acid and alkaline media. On the other hand, the SiM samples were homogeneous in terms of the

intensity of gold diffraction. This effect is related to smaller crystal sizes and better dispersions of the metal when compared to the IiM samples [47]. Therefore, the pH had an effect on the crystal size in the samples from the impregnation method.

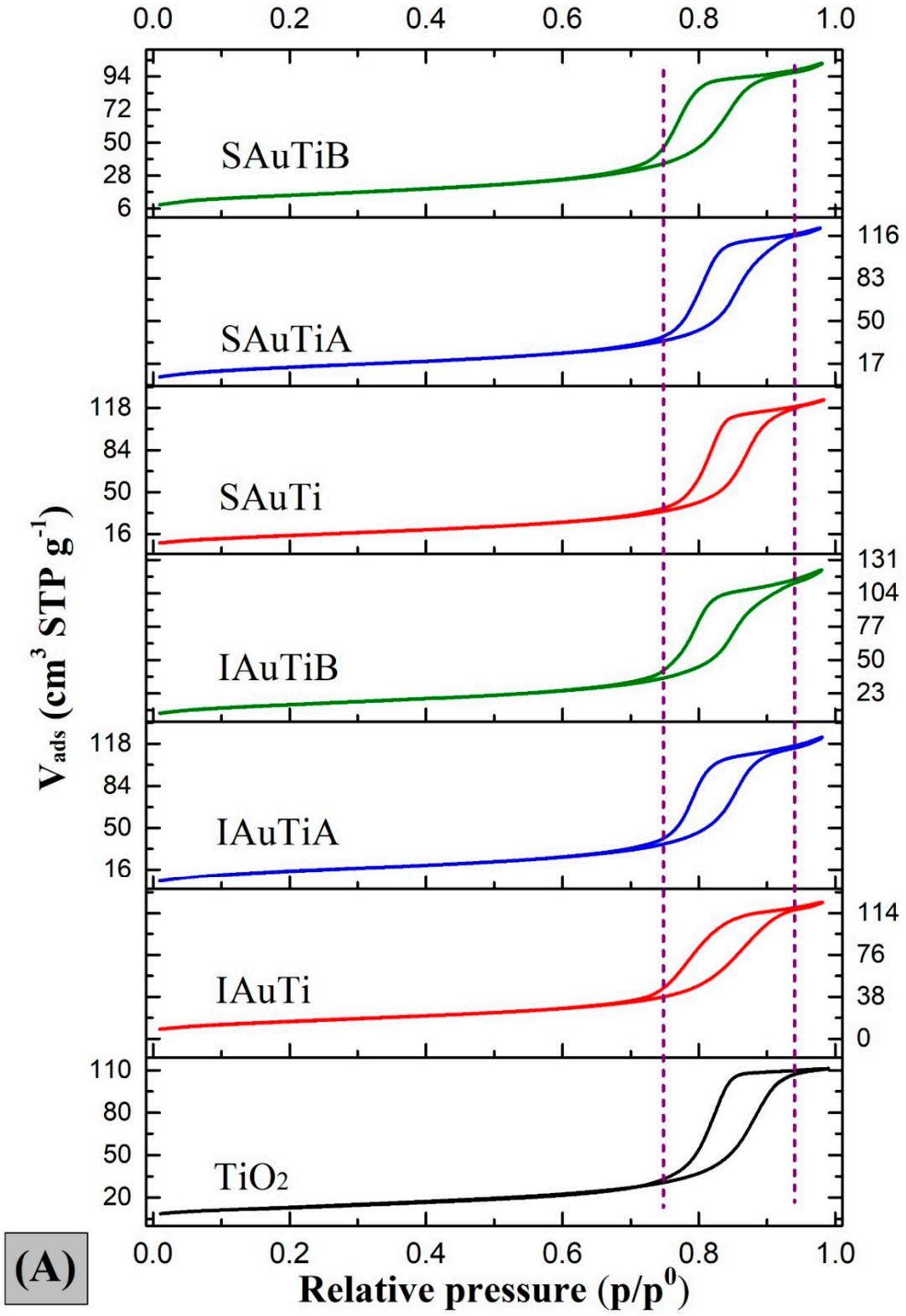

Figure 2. *Cont.*

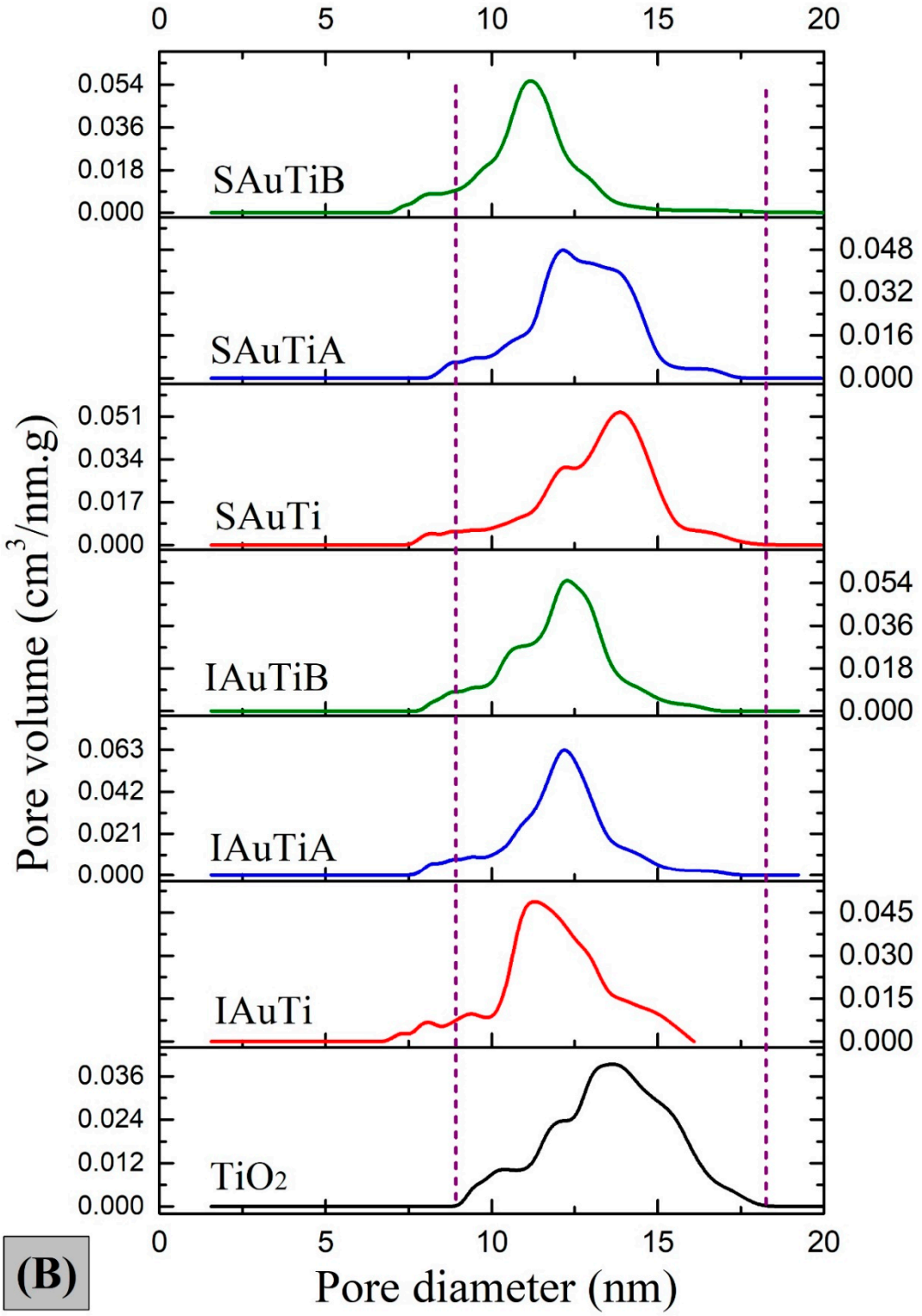

Figure 2. Nitrogen sorption results for Au/TiO_2 samples. (**A**) Sorption isotherms. (**B**) Average pore diameter by NLDFT.

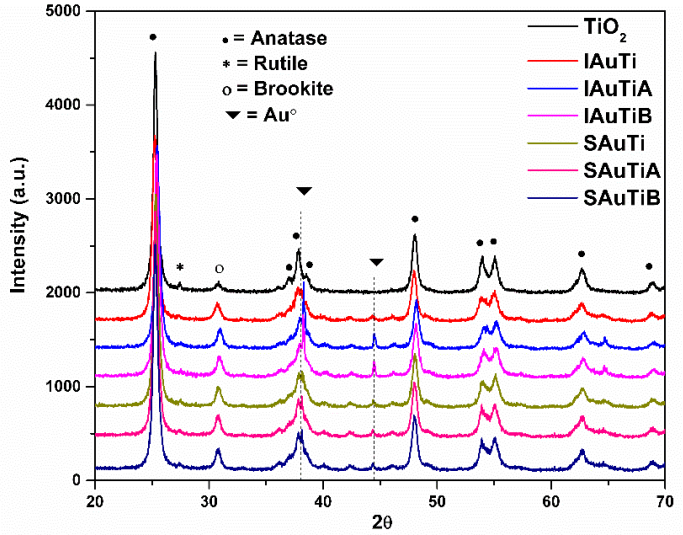

Figure 3. X-ray diffraction of the samples synthesized by "Suspension Impregnation Method" (SiM) and "Incipient Impregnation Method" (IiM).

The gold concentration in the samples is shown in Table 1. The concentration in the samples by IiM is close to the theoretical value (1% by weight) and there is little difference between them. However, the samples synthesized by SiM have lower concentrations, with a loss about 0.09%. This effect is due to the deposit of gold on the porous plate of the suspension system. This was evident by the observation of a purple coloration on the plate after the removal of the sample.

The results of thermogravimetric (TGA) and differential thermal (DTA) analyses are shown in Figure 4. The first one, at an interval of 25–200 °C, corresponds to the loss of water adsorbed on the surface of the material and surface hydroxylation. The second one at 200–300 °C corresponds to the loss of weight by the combustion of the remaining organic material [48]. Three processes with endothermic characteristics related to structural changes were also determined. The first, around 380 °C, corresponds to the formation of the anatomic structure of titanium oxide. The second, 580 °C, is the formation of rutile [48]. The third stage is related to the sintering of the gold particles at sizes of approximately 50 nm [49].

The thermal processes in the samples are congruent with the X-ray results. That is, the brookite structure was arranged in the anatase structure, associated with one of the thermal processes at 386 °C. At a higher energy, the anatase was rearranged into rutile (578 °C)—the second process. Finally, the metal present on the surface of the oxide was sintered at 863 °C.

To determine the distribution and average size of the metallic particles, the TEM technique was used; the results are shown in Figure 5. For this reason, the HAADF technique was used to contrast with the metal of the titanium oxide, see Figure 5F. According to the average particle size, the following order was determined: IAuTiB > SAuTiB > IAuTiA > IAuTi > SAuTi > SAuTiA. In relation to the size distribution, the SAuTi sample showed homogeneity with a high percentage of particles at 2 nm compared to IAuTi. This effect was similar when comparing IAuTA-SAuTiA and IAuTiB-SAuTiB. It is evident that SiM provides homogeneity in metal particle sizes with respect to those obtained by IiM. Using the concentration of metal by ICP and the mean diameter of the metal, the degree of metal dispersion was calculated, viz. Table 1. The "SiM" showed a better dispersion of the metal on the surface of the titanium oxide and improved further under acidic conditions.

The chemical phenomena in the synthesis of IiM indicate that the pH catalyzed the formation of different species of the precursor that directly affect the extension of the hydrolysis of the metallic precursor. The different metal precursors or their hydrolyzed counterparts have variable dimensions when, for example, the chloride ligand is changed to hydroxyl with an increase in pH [50]. According to the above, the material synthesized in an acidic medium had a pH of 3; therefore, the formation of

$AuCl_3(OH)$ species is highly likely [51]. In addition, the acidic pH from inorganic acids, such as HCl, possess the chloride ion, which promotes the polymerization of gold particles [29,52]. In contrast, the material synthesized in a basic medium with a pH of 7.5 favored the formation of $AuCl(OH)_3$-type species [51]. These species have a low stability and consequently a slow speed of surface adsorption [29]. Therefore, the short mixing times and the low concentration of the additives (HCl, Urea) allowed for the agglomeration of the particles. These parameters are in clear contrast to what has been reported in the literature [53,54]. The results of these synthesis conditions were reflected in the gold particle size.

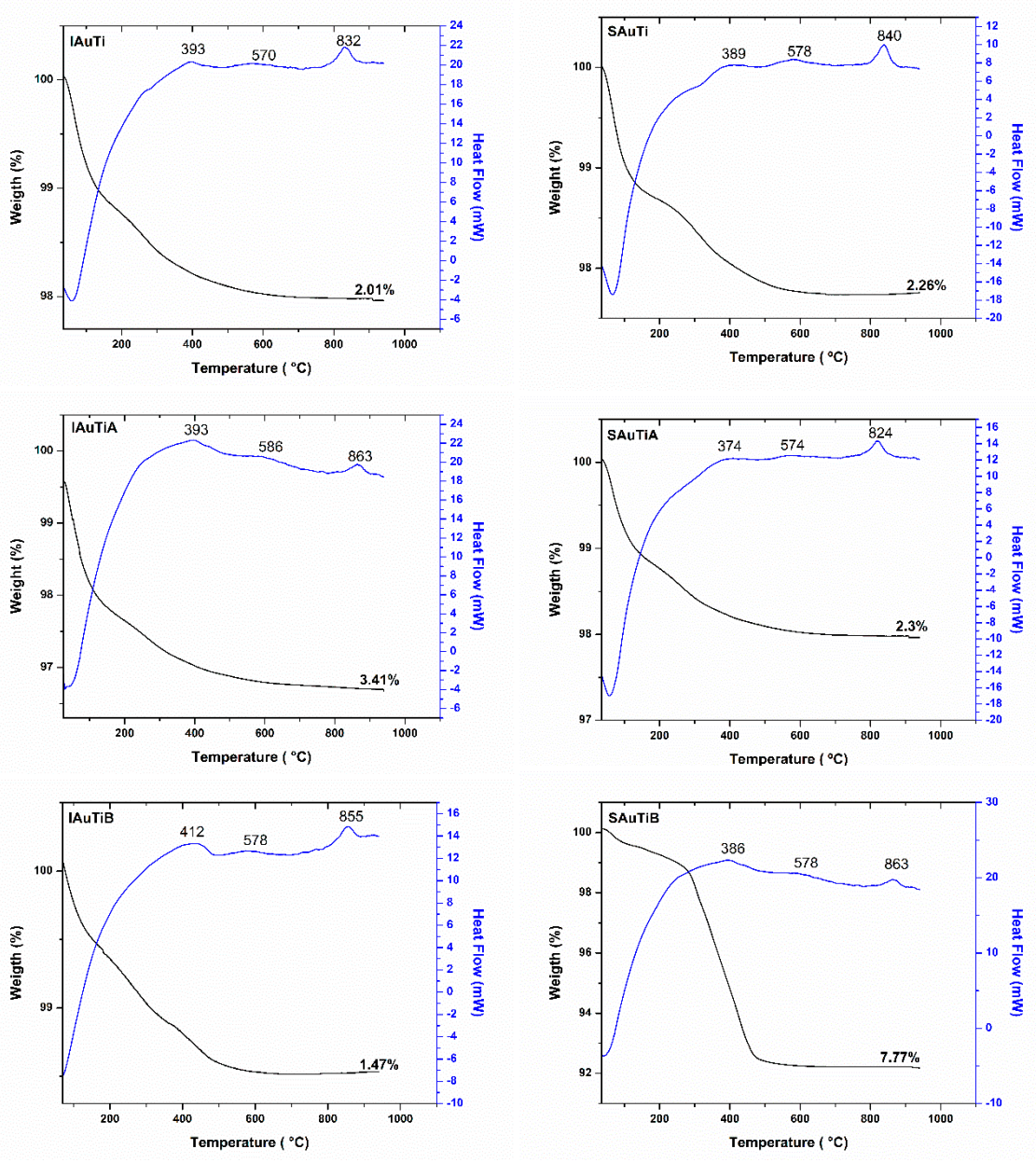

Figure 4. Thermogravimetric analysis of the materials synthesized by IiM and SiM.

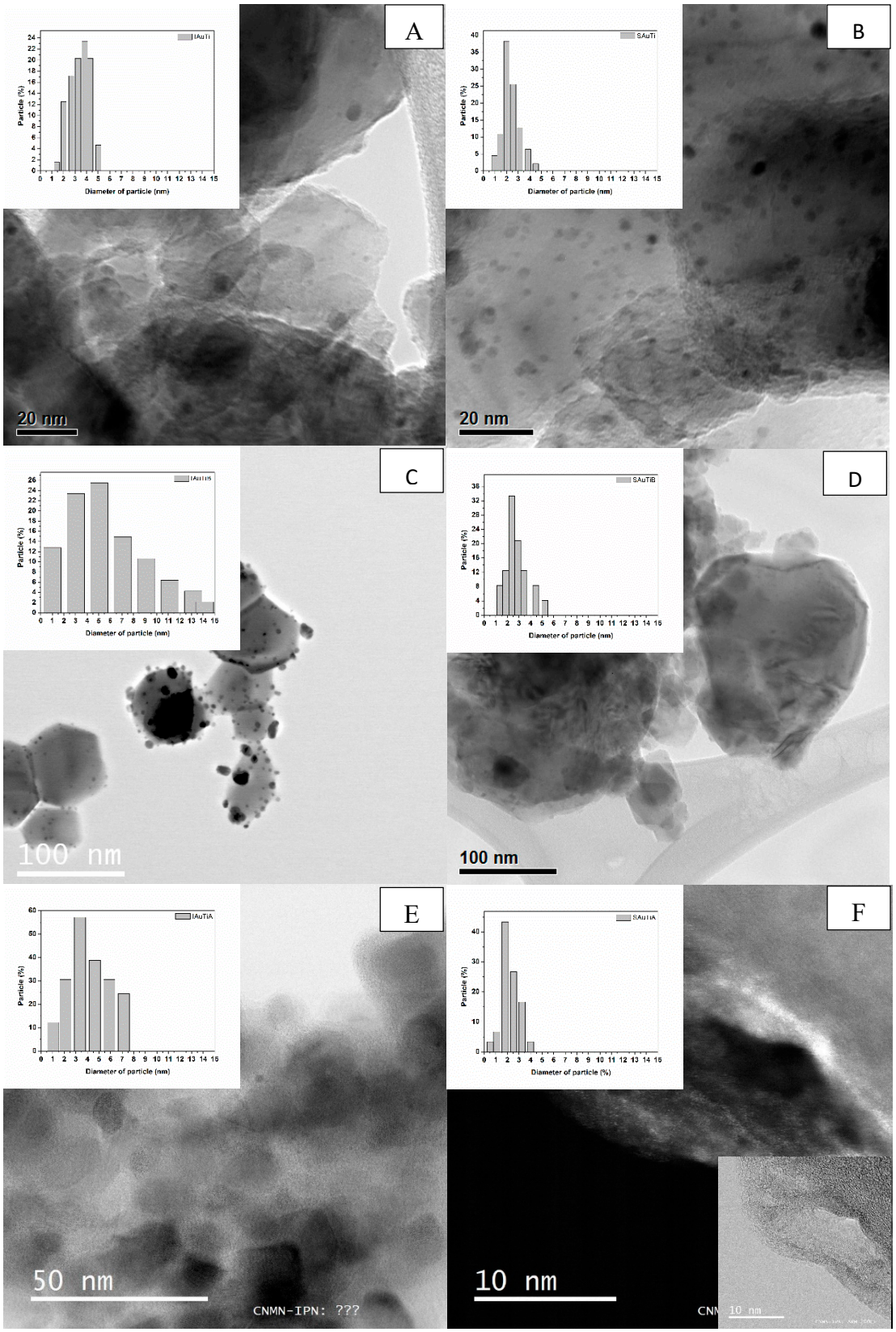

Figure 5. TEM images of the samples synthesized without pH modification by the IiM and SiM, (**A**,**B**), respectively. TEM images of the samples synthesized in basic pH by the IiM and SiM, (**C**,**D**), respectively. Samples synthesized in acid pH by the IiM and SiM, (**E**,**F**), respectively.

In the case of SiM, the basic principle is the direct reduction in the species formed within the liquid. According to thermodynamics, the species formed in the liquid can be reduced according to the chemical potentials, as shown in Equations (3) and (4).

$$AuCl_4^- + 3e^- \leftrightarrow Au + 4Cl^- \quad (3)$$

$$2H^+ + 2e^- \leftrightarrow H_2 \quad (4)$$

The difference in equilibrium potentials determines the value of the change in the free energy and, therefore, the direction of the overall reaction: $\Delta G = -Z_{Au}Z_H F(E_{Au} - E_H)$. If $E_{Au} > E_H$ the ΔG will be negative and therefore the oxidized form of Au will be reduced by the hydrogen. The standard chemical potential of the $AuCl^{4-}$ species is 1 V, while, by agreement, the standard hydrogen reduction potential is 0 V. Therefore, any species formed in solution will be reduced in the presence of hydrogen. Under these conditions, the presence of hydrogen prevented the formation of clusters and consequently smaller gold particles.

3.2. CO_2 Adsorption

The effect of the surface chemical activity obtained after impregnating TiO_2 with gold was studied using the CO_2 adsorption technique at 25 °C. CO_2 adsorption isotherms are shown in Figure 6. The adsorption capacity of the titanium oxide was favored by the incorporation of the metallic gold particles, rising up to eight times; however, this was not enough to make it an efficient material for CO_2 capture to compete with materials like SBA-15 [41], zeolites [37,38] or carbon [39,40]. According to the amount of CO_2, the order was: SAuTiA > SAuTiB > SAuTi > IAuTi > IAuTiA > IAuTiB > TiO_2. This allows us to say that the suspension method (SiM) is better than the impregnation method (IiM). Moreover, the acid medium improves the CO_2 adsorption.

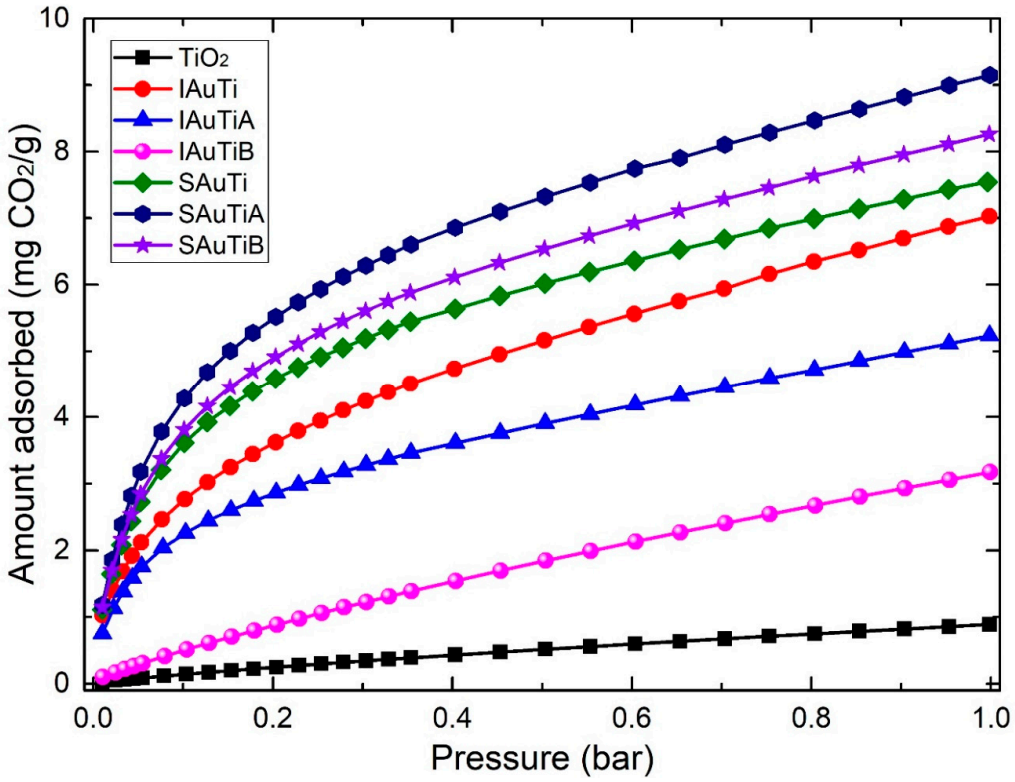

Figure 6. CO_2 adsorption isotherms at 25 °C for materials of TiO_2 doped with Au.

4. Conclusions

The suspension impregnation method was efficient in nanoparticle synthesis compared to the impregnation method. The structure of the titanium oxide was not altered after the metal was deposited. The surface area was slightly improved by the redispersion of the titanium oxide in solution. Based on the particle size calculated by TEM and the decrease in average pore size, it is likely that some pores have been covered by gold particles. A simple technique, such as CO_2 adsorption, allowed us to determine the effect of the chemical activity of the modified materials. In general, all of them increased their chemical nature, but the materials impregnated by the SiM technique generated more homogeneous materials with an increased activity towards CO_2 capture. The in situ reduction in the species formed by the pH influenced the particle size distribution, showing that the SiM method increases the homogeneity of the metal particle sizes. SiM is a promising technique for the deposition of noble metals that are difficult to disperse by other methods.

Author Contributions: Conceptualization, Á.E.G.-D.; data curation, F.G.-R.; funding acquisition, C.F.; investigation, C.R.-M.; methodology, A.S.-P.; resources, G.T.-T.; visualization, R.O.S.-D.; writing—original draft, A.C.-U.; writing—review & editing, R.O.-L. All authors have read and agreed to the published version of the manuscript.

Funding: This research was supported by the Secretaria de Investigación y Posgrado (IPN) under project 20,200,829: "Síntesis de materiales nanoporosos y la simulación por métodos de Monte Carlo de los procesos capilares ocurrentes en sus nanocavidades".

Acknowledgments: Carolina Rodríguez Martínez thanks the DRX laboratory (INFR-2011-1-163250) in the Universidad Autónoma Metropolitana and the Microscopía Electrónica de Transmisión in the Instituto Politécnico Nacional.

Conflicts of Interest: The authors declare that they have no known competing financial interests or personal relationships that may appear to influence the work reported in this paper.

References

1. Valden, M.; Pak, S.; Lai, X.; Goodman, D.W. Structure sensitivity of CO oxidation over model Au/TiO_2 catalysts. *Catal. Lett.* **1998**, *56*, 7–10. [CrossRef]
2. van Bokhoven, J.A.; Louis, C.; Miller, J.T.; Tromp, M.; Safonova, O.V.; Glatzel, P. Activation of Oxygen on Gold/Alumina Catalysts: In Situ High-Energy-Resolution Fluorescence and Time-Resolved X-ray Spectroscopy. *Angew. Chem.* **2006**, *118*, 4767–4770. [CrossRef]
3. Mavrikakis, M.; Stoltze, P.; Nørskov, J.K. Making gold less noble. *Catal. Lett.* **2000**, *64*, 101–106. [CrossRef]
4. Janssens, T.V.W.; Clausen, B.S.; Hvolbæk, B.; Falsig, H.; Christensen, C.H.; Bligaard, T.; Nørskov, J.K. Insights into the reactivity of supported Au nanoparticles: Combining theory and experiments. *Top. Catal.* **2007**, *44*, 15–26. [CrossRef]
5. Abutalib, M.M.; Rajeh, A. Influence of ZnO/Ag nanoparticles doping on the structural, thermal, optical and electrical properties of PAM/PEO composite. *Phys. B Condens. Matter* **2020**, *578*, 411796. [CrossRef]
6. Chen, S.; Chang, A.; Rungsi, A.N.; Attanatho, L.; Chang, C.; Pan, J.; Suemanotham, A.; Mochizuki, T.; Takagi, H.; Yang, C.; et al. Superficial Pd nanoparticles supported on carbonaceous SBA-15 as efficient hydrotreating catalyst for upgrading biodiesel fuel. *Appl. Catal. A Gen.* **2020**, 117707. [CrossRef]
7. Li, J.; Yuan, R.; Chai, Y.; Che, X. Fabrication of a novel glucose biosensor based on Pt nanoparticles- decorated iron oxide-multiwall carbon nanotubes magnetic composite. *J. Mol. Catal. B Enzym.* **2010**, *66*, 8–14. [CrossRef]
8. Li, Y.; Sundermann, A.; Gerlach, O.; Low, K.B.; Zhang, C.C.; Zheng, X.; Zhu, H.; Axnanda, S. Catalytic decomposition of N_2O on supported Rh catalysts. *Catal. Today* **2019**. [CrossRef]
9. Srimara, P.; Chevapruk, T.; Kumnorkaew, P.; Muangnapoh, T.; Vas-Umnuay, P. Synthesis of Ni Nanoparticles for Solar Selective Absorber by Chemical Reduction Method. *Mater. Today Proc.* **2020**, *23*, 720–725. [CrossRef]
10. Haruta, M.; Kobayashi, T.; Sano, H.; Yamada, N. Novel Gold Catalysts for the Oxidation of Carbon Monoxide at a Temperature far Below 0 °C. *Chem. Lett.* **1987**, *16*, 405–408. [CrossRef]
11. Valden, M.; Lai, X.; Goodman, D.W. Onset of catalytic activity of gold clusters on titania with the appearance of nonmetallic properties. *Science* **1998**, *281*, 1647–1650. [CrossRef]

12. Yoshida, T.; Misu, Y.; Yamamoto, M.; Tanabe, T.; Kumagai, J.; Ogawa, S.; Yagi, S. Effects of the amount of Au nanoparticles on the visible light response of TiO_2 photocatalysts. *Catal. Today* **2020**, *352*, 34–38. [CrossRef]
13. Portillo-Vélez, N.S.; Zanella, R. Comparative study of transition metal (Mn, Fe or Co) catalysts supported on titania: Effect of Au nanoparticles addition towards CO oxidation and soot combustion reactions. *Chem. Eng. J.* **2020**, *385*, 123848. [CrossRef]
14. Khdary, N.H.; Ghanem, M.A.; Merajuddine, M.G.; Bin Manie, F.M. Incorporation of Cu, Fe, Ag, and Au nanoparticles in mercapto-silica (MOS) and their CO_2 adsorption capacities. *J. CO_2 Util.* **2014**, *5*, 17–23. [CrossRef]
15. Du, L.; Furube, A.; Yamamoto, K.; Hara, K.; Katoh, R.; Tachiya, M. Plasmon-induced charge separation and recombination dynamics in gold-TiO_2 nanoparticle systems: Dependence on TiO_2 particle size. *J. Phys. Chem. C* **2009**, *113*, 6454–6462. [CrossRef]
16. Wang, S.; Wang, Y.; Jiang, J.; Liu, R.; Li, M.; Wang, Y.; Su, Y.; Zhu, B.; Zhang, S.; Huang, W.; et al. A DRIFTS study of low-temperature CO oxidation over Au/SnO_2 catalyst prepared by co-precipitation method. *Catal. Commun.* **2009**, *10*, 640–644. [CrossRef]
17. Haruta, M.; Tsubota, S.; Kobayashi, T.; Kageyama, H.; Genet, M.J.; Delmon, B. Low-temperature oxidation of CO over gold supported on TiO_2, α-Fe_2O_3, and Co_3O. *J. Catal.* **1993**, *144*, 175–192. [CrossRef]
18. Okumura, M.; Tanaka, K.; Ueda, A.; Haruta, M. The reactivities of dimethylgold(III)β-diketone on the surface of TiO_2 A novel preparation method for Au catalysts. *Solid State Ion.* **1997**, *95*, 143–149. [CrossRef]
19. Li, J.; Zeng, H.C. Preparation of Monodisperse Au/TiO_2 Nanocatalysts via Self-Assembly. *Chem. Mater.* **2006**, *18*, 4270–4277. [CrossRef]
20. Deki, S.; Aoi, Y.; Yanagimoto, H.; Ishii, K.; Akamatsu, K.; Mizuhata, M.; Kajinami, A. Preparation and characterization of Au-dispersed TiO_2 thin films by a liquid-phase deposition method. *J. Mater. Chem.* **1996**, *6*, 1879–1882. [CrossRef]
21. Yang, Y.F.; Sangeetha, P.; Chen, Y.W. Au/TiO_2 catalysts prepared by photo-deposition method for selective CO oxidation in H_2 stream. *Int. J. Hydrog. Energy* **2009**, *34*, 8912–8920. [CrossRef]
22. Sonawane, R.S.; Dongare, M.K. Sol-gel synthesis of Au/TiO_2 thin films for photocatalytic degradation of phenol in sunlight. *J. Mol. Catal. A Chem.* **2006**, *243*, 68–76. [CrossRef]
23. Kim, M.Y.; Park, J.H.; Shin, C.H.; Han, S.W.; Seo, G. Dispersion improvement of platinum catalysts supported on silica, silica-alumina and alumina by titania incorporation and ph adjustment. *Catal. Lett.* **2009**, *133*, 288–297. [CrossRef]
24. Toebes, M.L.; Van Der Lee, M.K.; Tang, L.M.; In 'T Veld, M.H.H.; Bitter, J.H.; Van Dillen, A.J.; De Jong, K.P. Preparation of carbon nanofiber supported platinum and ruthenium catalysts: Comparison of ion adsorption and homogeneous deposition precipitation. *J. Phys. Chem. B* **2004**, *108*, 11611–11619. [CrossRef]
25. Oh, H.S.; Oh, J.G.; Kim, H. Modification of polyol process for synthesis of highly platinum loaded platinum-carbon catalysts for fuel cells. *J. Power Sources* **2008**, *183*, 600–603. [CrossRef]
26. Zanella, R.; Delannoy, L.; Louis, C. Mechanism of deposition of gold precursors onto TiO_2 during the preparation by cation adsorption and deposition-precipitation with NaOH and urea. *Appl. Catal. A Gen.* **2005**, *291*, 62–72. [CrossRef]
27. Phonthammachai, N.; White, T.J. One-step synthesis of highly dispersed gold nanocrystals on silica spheres. *Langmuir* **2007**, *23*, 11421–11424. [CrossRef]
28. Tsoncheva, T.; Gallo, A.; Scotti, N.; Dimitrov, M.; Delaigle, R.; Gaigneaux, E.M.; Kovacheva, D.; Dal Santo, V.; Ravasio, N. Optimization of the preparation procedure of cobalt modified silicas as catalysts in methanol decomposition. *Appl. Catal. A Gen.* **2012**, *417–418*, 209–219. [CrossRef]
29. Ivanova, S.; Pitchon, V.; Petit, C.; Herschbach, H.; Van Dorsselaer, A.; Leize, E. Preparation of alumina supported gold catalysts: Gold complexes genesis, identification and speciation by mass spectrometry. *Appl. Catal. A Gen.* **2006**, *298*, 203–210. [CrossRef]
30. Baatz, C.; Thielecke, N.; Prüße, U. Influence of the preparation conditions on the properties of gold catalysts for the oxidation of glucose. *Appl. Catal. B Environ.* **2007**, *70*, 653–660. [CrossRef]
31. Schaal, M.T.; Rebelli, J.; McKerrow, H.M.; Williams, C.T.; Monnier, J.R. Effect of liquid phase reducing agents on the dispersion of supported Pt catalysts. *Appl. Catal. A Gen.* **2010**, *382*, 49–57. [CrossRef]
32. Saunders, A.E.; Sigman, M.B.; Korgel, B.A. Growth kinetics and metastability of monodisperse TOAB capped Au. *JPCB* **2004**, *108*, 193–199. [CrossRef]

33. Miller, J.T.; Schreier, M.; Kropf, A.J.; Regalbuto, J.R. A fundamental study of platinum tetraammine impregnation of silica: The effect of method of preparation, loading, and calcination temperature on (reduced) particle size. *J. Catal.* **2004**, *225*, 203–212. [CrossRef]
34. Girardon, J.S.; Quinet, E.; Griboval-Constant, A.; Chernavskii, P.A.; Gengembre, L.; Khodakov, A.Y. Cobalt dispersion, reducibility, and surface sites in promoted silica-supported Fischer-Tropsch catalysts. *J. Catal.* **2007**, *248*, 143–157. [CrossRef]
35. Maitra, A.M.; Cant, N.W.; Trimm, D.L. The Preparation of Tungten Based. *Appl. Catal.* **1986**, *27*, 9–19. [CrossRef]
36. Boccuzzi, F.; Chiorino, A.; Martra, G.; Gargano, M.; Ravasio, N.; Carrozzini, B. Preparation, characterization, and activity of Cu/TiO_2 catalysts: I. Influence of the preparation method on the dispersion of copper in Cu/TiO. *J. Catal.* **1997**, *165*, 129–139. [CrossRef]
37. Bezerra, D.P.; Silva, F.W.M.D.; Moura, P.A.S.D.; Sousa, A.G.S.; Vieira, R.S.; Rodriguez-Castellon, E.; Azevedo, D.C.S. CO_2 adsorption in amine-grafted zeolite 13X. *Appl. Surf. Sci.* **2014**, *314*, 314–321. [CrossRef]
38. Liu, L.; Du, T.; Li, G.; Yang, F.; Che, S. Using one waste to tackle another: Preparation of a CO_2 capture material zeolite X from laterite residue and bauxite. *J. Hazard. Mater.* **2014**, *278*, 551–558. [CrossRef]
39. Ojeda-López, R.; Aguilar-Huerta, E.; Maia, D.; Azevedo, D.; Felipe, C.; Domíngez-Ortiz, A. Tailoring synthesis conditions of carbon microfibers to enhance the microporosity, CO_2 and CH_4 adsorption by using the response surface methodology. *Microporous Mesoporous Mater.* **2020**, *305*, 110333–110341. [CrossRef]
40. Ojeda-López, R.; Esparza-Schulz, J.M.; Pérez-Hermosillo, I.J.; Hernández-Gordillo, A.; Domínguez-Ortiz, A. Improve in CO_2 and CH_4 Adsorption Capacity on Carbon Microfibers Synthesized by Electrospinning of PAN. *Fibers* **2019**, *7*, 81. [CrossRef]
41. Ojeda-López, R.; Pérez-Hermosillo, I.J.; Marcos Esparza-Schulz, J.; Cervantes-Uribe, A.; Domínguez-Ortiz, A. SBA-15 materials: Calcination temperature influence on textural properties and total silanol ratio. *Adsorption* **2015**, *21*, 659–669. [CrossRef]
42. Gmachowski, L. Gmachowski1996.Pdf. *J. Chem. Eng. Jpn.* **1996**, *29*, 897–900. [CrossRef]
43. Thommes, M.; Kaneko, K.; Neimark, A.V.; Olivier, J.P.; Rodriguez-Reinoso, F.; Rouquerol, J.; Sing, K.S.W. Physisorption of gases, with special reference to the evaluation of surface area and pore size distribution (IUPAC Technical Report). *Pure Appl. Chem.* **2015**, *87*, 1051–1069. [CrossRef]
44. Musić, S.; Gotić, M.; Ivanda, M.; Popović, S.; Turković, A.; Trojko, R.; Sekulić, A.; Furić, K. Chemical and microstructural properties of TiO2 synthesized by sol-gel procedure. *Mater. Sci. Eng. B* **1997**, *47*, 33–40. [CrossRef]
45. Hanaor, D.A.H.; Chironi, I.; Karatchevtseva, I.; Triani, G.; Sorrell, C.C. Single and mixed phase TiO_2 powders prepared by excess hydrolysis of titanium alkoxide. *Adv. Appl. Ceram.* **2012**, *111*, 149–158. [CrossRef]
46. Silahua-Pavón, A.A.; Torres-Torres, G.; Arévalo-Pérez, J.C.; Cervantes-Uribe, A.; Guerra-Que, Z.; Cordero-García, A.; Espinosa de Los Monteros, A.; Beltramini, J.N. Effect of gold addition by the recharge method on silver supported catalysts in the catalytic wet air oxidation (CWAO) of phenol. *RSC Adv.* **2019**, *9*, 11123–11134. [CrossRef]
47. Padikkaparambil, S.; Narayanan, B.; Yaakob, Z.; Viswanathan, S.; Tasirin, S.M. Au/TiO_2 reusable photocatalysts for dye degradation. *Int. J. Photoenergy* **2013**, *2013*. [CrossRef]
48. Jane Huang, P.; Chang, H.; Tih Yeh, C.; Wen Tsai, C. Transformation of TiO_2 monitored by Thermo-Raman spectroscopy with TGA/DTA. *Thermochimca Acta* **1997**, *297*, 85–92. [CrossRef]
49. Lee, I.; Joo, J.B.; Yin, Y.; Zaera, F. A yolk@shell nanoarchitecture for Au/TiO_2 catalysts. *Angew. Chem. Int. Ed.* **2011**, *50*, 10208–10211. [CrossRef]
50. Souza, K.R.; de Lima, A.F.F.; de Sousa, F.F.; Appel, L.G. Preparing Au/ZnO by precipitation-deposition technique. *Appl. Catal. A Gen.* **2008**, *340*, 133–139. [CrossRef]
51. Moreau, F.; Bond, G.C.; Taylor, A.O. Gold on titania catalysts for the oxidation of carbon monoxide: Control of pH during preparation with various gold contents. *J. Catal.* **2005**, *231*, 105–114. [CrossRef]
52. Yang, J.H.; Henao, J.D.; Costello, C.; Kung, M.C.; Kung, H.H.; Miller, J.T.; Kropf, A.J.; Kim, J.G.; Regalbuto, J.R.; Bore, M.T.; et al. Understanding preparation variables in the synthesis of Au/Al_2O_3 using EXAFS and electron microscopy. *Appl. Catal. A Gen.* **2005**, *291*, 73–84. [CrossRef]

53. Aboukaïs, A.; Aouad, S.; El-Ayadi, H.; Skaf, M.; Labaki, M.; Cousin, R.; Abi-Aad, E. Catalytic oxidation of propylene, toluene, carbon monoxide, and carbon black over Au/CeO_2 solids: Comparing the impregnation and the deposition-precipitation methods. *Sci. World J.* **2013**, *2013*. [CrossRef] [PubMed]
54. Leal, G.B.; Ciotti, L.; Watacabe, B.N.; Loureiro da Silva, D.C.; Antoniassi, R.M.; Silva, J.C.M.; Linardi, M.; Giudici, R.; Vaz, J.M.; Spinacé, E.V. Preparation of Au/TiO_2 by a facile method at room temperature for the CO preferential oxidation reaction. *Catal. Commun.* **2018**, *116*, 38–42. [CrossRef]